1

Establishment of the effectiveness of early versus late stem cell gene therapy in mucopolysaccharidosis II for treating central versus peripheral disease

Oriana Mandolfo[1*], Aiyin Liao[1], Esha Singh[1], Claire O'leary[1], Rebecca J. Holley[1] and Brian W. Bigger[1]

[1]*Stem Cell and Neurotherapies, Faculty of Biology, Medicine and Health, University of Manchester, Manchester, UK*

Correspondence should be addressed to B.W.B. (brian.bigger@manchester.ac.uk)

Corresponding author: Professor Brian Bigger, Stem Cell and Neurotherapies, Division of Cell Matrix Biology and Regenerative Medicine, Faculty of Biology, Medicine and Health, 3.721 Stopford Building, Oxford Road, University of Manchester, Manchester, M13 9PT. UK. Tel: 0161 306 0516. Email: brian.bigger@manchester.ac.uk

Short title: Reversibility in MPSII

2

Abstract

Mucopolysaccharidosis type II (MPSII) is a rare paediatric X-linked lysosomal storage disease, caused by heterogeneous mutations in the IDS gene, which result in accumulation of heparan sulphate and dermatan sulphate within cells. This leads to severe skeletal abnormalities, hepatosplenomegaly and cognitive deterioration. The progressive nature of the disease is a huge obstacle to achieve full neurological correction. Although current therapies can only treat somatic symptoms, a lentivirus-based hematopoietic stem cell gene therapy (HSCGT) approach has recently achieved improved central nervous system neuropathology in the MPSII mouse model following transplant at 2-months of age. Here we evaluate neuropathology progression in 2-month, 4-month and 9-month-old MPSII mice and using the same HSCGT strategy we investigated somatic and neurological disease attenuation following treatment at 4-months of age. Our results showed gradual accumulation of heparan sulphate between 2 and 4 months of age, but full manifestation of microgliosis/astrogliosis as early as 2 months. Late HSCGT fully reversed the somatic symptoms, thus achieving the same degree of peripheral correction as early therapy. However, late treatment resulted in slightly decreased efficacy in the CNS, with poorer brain enzymatic activity, together with reduced normalisation of heparan sulphate over-sulphation. Overall, our findings confirm significant lysosomal burden and neuropathology in 2-month-old MPSII mice. Peripheral disease is readily reversible by LV.IDS-HSCGT regardless of age of transplant, suggesting a viable treatment for somatic disease. However, in the brain, higher IDS enzyme levels are achievable with early HSCGT treatment, and later transplant seems to be less effective, supporting the view that the earlier patients are diagnosed and treated, the better the therapy outcome.

3

Introduction

Lysosomal storage diseases (LSDs) are a group of about 70 disorders that arise mainly from inherited mutations in the genes encoding the proteins responsible for lysosomal catabolism. One group of LSDs is the mucopolysaccharidoses (MPS) family, which has a frequency of about 1 in 7500 live-births[1], whose sufferers carry defects in the genes involved in the degradation of glycosaminoglycans (GAGs). MPS type II, known as Hunter disease, is caused by defects in the X-linked gene IDS, encoding the hydrolase enzyme iduronate 2-sulphatase (I2S) which is essential for the degradation of both heparan sulphate (HS) and dermatan sulphate (DS)[2]. As a result, I2S deficiency leads to progressive accumulation of these unmetabolized molecules in cells and tissues, eventually resulting in a chronic multisystemic disease. MPSII is generally classified into an attenuated and severe form, although disease symptoms manifest as a continuum between the two extremes[3]. Patients usually experience a wide range of somatic symptoms, including skeletal abnormalities, limited joint motility, airway and pulmonary restriction, cardiomyopathy and hepatosplenomegaly. In addition to these, the severe disease form is also marked by central nervous system (CNS) involvement, characterised by progressive cognitive deterioration, hyperactivity, aggression and sleep disturbances, with life expectancy often not exceeding the first decade of life[4].

Currently, enzyme replacement therapy (ERT) is the only approved therapeutic approach for MPSII. This consists of weekly intravenous administrations of idursulfase or idursulfase beta, a formulation containing recombinant I2S enzyme, which is internalised by cells via mannose-6-phosphate (M6P) receptor-mediated endocytosis[5]. ERT is particularly effective in ameliorating the somatic symptoms of MPSII, especially at the musculoskeletal and visceral organs level, increasing the quality of life for many patients. However, this strategy fails to treat the neurological symptoms associated with severe MPSII, due to the inability of the enzyme to cross the blood-brain barrier (BBB)[6].

Haematopoietic stem cell therapy (HSCT) is able to provide correction of the brain in related disease MPSI, although has limited efficacy in other MPS subtypes[7]. This therapy involves the infusion of haematopoietic stem cells (HSC) derived from matched healthy donors into

4

patients that have received full myeloablative conditioning. Following engraftment in the bone marrow, a small proportion of donor-derived myeloid cells seems to be able to migrate, cross the BBB and engraft as microglia-like cells, eventually secreting enzyme for cross-correction in the brain[8–12]. A recent study has showed that HSCT can partially ameliorate both motor and speech skills in MPSII patients up to 7 years of age post-transplant[13]; however results are poor compared to the efficacy achieved in MPSI patients, presumably due to HSCT failing to achieve the required threshold level of I2S enzyme in the brain.

Although, there is evidence suggesting that HSCT may stabilise cognition in MPSII patients if transplant is given at early disease stages[14], the levels of enzyme provided by a healthy donor remain a limiting factor to achieve complete neurological correction[15]. In this respect, haematopoietic stem cell gene therapy (HSCGT) represents a promising alternative for MPSII treatment, as the patient's HSCs are genetically modified to over-express the missing enzyme prior delivery, eventually overcoming the threshold limit of enzyme required in the brain[16,17]. Encouraging results were achieved following lentiviral-mediated HSCGT in mouse models of MPS II, IIIA and IIIB[10–12,18]. With regards to MPSII, the ability of somatic IDS enzyme to cross the BBB was enhanced by fusing the codon-optimised *IDS* to the receptor-binding domain of human apolipoprotein E (ApoE) cloned into a third-generation lentiviral vector containing the myeloid-specific CD11b promoter (LV.IDS.ApoEII). 2-month-old MPSII mice were transplanted with HSC transduced with either LV.IDS.ApoEII or the same lentivirus expressing normal IDS (LV.IDS). Although both treatments led to complete correction of somatic defects, only LV.IDS.ApoEII mediated complete normalization of brain pathology and spatial working memory deficits, providing significantly enhanced correction compared to LV.IDS. Nevertheless, LV.IDS still led to significant enzyme levels in the brain, with subsequential reductions in CNS HS and normalisation of sensorimotor coordination[11].

Despite these positive outcomes, the efficacy of any HSCGT approach to reverse neuropathology is highly dependent on the level of existing damage at the time of treatment. As a result, determining the time course of neurological deterioration becomes crucial for understanding the right time of therapeutic intervention for severe MPSII patients. Using the MPSII mouse model we set out to determine the degree of brain HS storage and neuropathology in 2- (young), 4- (middle-aged) and 9-month (old) animals.

5

Having established background levels of neuroinflammation we investigated the efficacy of HSCGT using LV.IDS performed in 4-month old animals and compared results to our previous study where animals were treated at 2-months of age[11].

Materials and methods

LV.IDS production

A third-generation lentiviral vector containing codon-optimised human IDS pCCL.sin.cPPT.hCD11b.IDS.wpre was cloned, produced in HEK293T cells and titrated as described[11].

Mice, HSC isolation, lentiviral transduction and transplantation

Mice on a C57BL/6 (CD45.2) or Pep3 CD45.1 congenic background were bred as described[11] and housed under 12/12-hour light/dark cycles with food and water provided *ad libitum* in individually ventilated cages in groups of 3-5 per cage. Only male wildtype or MPSII animals were used for experiments. All *in vivo* procedures were performed in accordance with the Animal (Scientific Procedures) Act, 1986 (UK) under home office licence P0C3AEEB0 and approved by the University of Manchester Animal Welfare and Ethical Review Body committee. Control age matched 2-, 4- and 9-month animals (n=4-8 per group) were used for comparison studies. Prior to transplantation bone marrow was isolated from CD45.1-MPSII mice, lineage depleted, and HSCs transduced with an MOI of 60 as described previously[19]. 4-month-old male MPS II mice were myeloablated using 125 mg/kg busulfan divided into 5 daily doses via intraperitoneal injection. On day 6 mice received 3×10^5 lineage-depleted LV.IDS-transduced HSCs via tail vein injection. Donor chimerism in peripheral blood was performed at 6-months of age/2 months post-transplant as described[12,19]. If chimerism was measured below 60%, animals were excluded from the study. X-rays were performed on anaesthetised live mice at 8-months of age using the Bruker In-Vivo Xtreme system, as previously described[11]. X-ray images were analyzed using ImageJ software for individual bones widths.

6

Behavioural analyses

At 8-months of age, motor coordination and balance were measured using the accelerating rotarod. Three trials were performed for a maximum of 300 seconds per test, with an average of all three trials recorded. Latency to fall was recorded as a percentage of total trial time as described[20]. The Y-maze was used to assess spatial working memory. Mice at 8-months of age were placed in a Y-maze consisting of three identical arms for 10 minutes. Entry into each arm with all four paws was noted and analysed as previously described[20].

Harvesting animals and tissue analysis

At harvest mice were anesthetised and transcardially perfused with PBS. One brain hemisphere was fixed in 4% paraformaldehyde for 24 hours transferred to 30% sucrose/2 mmol/l MgCl$_2$/PBS for 48 hours before freezing at -80°C. Samples of brain, spleen, liver, heart, lung, and kidney were snap frozen on dry ice. Bone marrow samples were collected by flushing the tibia and femur with 2% FBS/PBS followed by red blood cell lysis and storage of the cell pellet at -80°C. Blood samples were taken into citrate buffer on ice and spun at 200 x g to isolate plasma. Red blood cells were lysed, and remaining cells pelleted for storage at -80°C.

For enzyme assays samples of organs were ground in homogenisation buffer (0.5 M NaCL, 0.02 M Tris, 0.1% Triton X-100, pH7) and centrifuged at 5000 x g to isolate the supernatant. Starting material was standardized to 40 µg of total protein for liver, heart, lung, spleen, and bone marrow, and 60 µg for brain using Pierce BCA assay kit (ThermoFisher). IDS enzyme levels were determined as previously described[11] and the assay was standardised to WT values to normalise the variability between each assay run. Genomic DNA was isolated from samples of organs using the GenElute Mammalian Genomic DNA miniprep kit (Sigma) and vector copy number determined using quantitative PCR as described[19].

HS composition and amounts were determined in frozen tissues as described[12]. Immunohistochemisty for isolectin-B4, LAMP2, and GFAP was performed on free-floating coronal brain sections and imaged as described[12]. Quantification of percentage area stained was performed by thresholding in Image J using the following regions: for cortical regions, images from layers IV/V/VI at 0.14, -0.82 and -1.7 relative to Bregma were quantified and

7

averaged; for striatal quantification images from 0.14 and -0.82 relative to Bregma were quantified and averaged; hippocampus CA3 regions at -1.7 relative to Bregma was used; amygdala regions from -1.7 relative to Bregma were quantified.

Experimental design

For time-course analysis independent 2-. 4- and 9-month-old animals were harvested at the indicated time point (n=4/group for 2- and 4-month groups, and n=14 for 9-month animals). For transplant analysis data HSCGT was performed at 4-months of age in n=8 animals and directly compared to a previous study performed at 2-months of age[11]. Control animals (n=8 per group, WT and MPSII) were taken independently during this study and combined with controls (n-6 per group) used in the previous study[11].

Blinding *in vivo* treatment groups was impossible due to the nature of the transplant procedure performed and the severity in phenotype of the mouse model, with transplants staggered over several months due to recipient/donor availability. However, all analysis where possible was performed in a blinded fashion to avoid bias.

Statistical analysis

GraphPad Prism was used for one-way or two-way analysis of variance (ANOVA) and Tukey post hoc test for analysis. Significance was taken at $P<0.05\%$.

Results

Significant central pathology is present by 2 months of age with marked HS storage

To determine the degree of neuropathology and disease progression in MPSII, brain HS accumulation and pathology was investigated in WT and MPSII mice at 2-, 4-, and 9-months of age (Fig 1).

Significant HS accumulation was observed over WT by 2 months of age with 5-fold more HS in the brain of MPSII mice. Between 2- and 4-months, a significant doubling in HS was observed in MPSII mice, with 10-fold increases in HS over WT by 4-months of age. A plateau in maximum accumulation was recorded between 4- and 9-months of age, with no further increases in HS levels (Fig 1A). Analysis of the HS composition in MPSII groups revealed that

8

greater than 30% of brain HS was represented by fully sulphated ΔHexA(2S)-GlcNS(6S), compared to 14% in wild-type mice. While a trend towards further increases in more sulphated disaccharides versus decreases in non-/low-sulphated disaccharide species was seen between 2- and 9-month MPSII animals, these were not significant (Fig 1B). This suggests that the pathological alterations in HS patterning occur prior to 2-months of age in MPSII animals.

Microglia form an important immune function in the brain, with their activation a hallmark of disease pathology. To assess neuro-inflammation, isolectin B4 (ISB4) staining was performed. In WT animals a few activated microglial cells were visible in cortex regions at all ages studied (Fig 1C), with little staining in other regions of the brain (Fig S1). Conversely significant microgliosis was present in MPSII animals in all regions of the brain studied (Fig 1C and S1). Quantification indicated that no significant differences were present between 2-, 4- and 9-month animals (Fig 1E). Co-staining for lysosomal swelling (lysosomal associated membrane protein-2; LAMP2) and astrogliosis (glial fibrillary associated protein; GFAP) and quantification revealed extensive LAMP2 and GFAP staining present at 2-months of age in MPSII animals (Fig 1D). A trend towards increased astrogliosis was indicated between 2- and 9-month animals, although this was not significant (Fig 1G). Conversely, lysosomal size was significantly increased by 1.6-fold between 4- and 9-months of age (Fig 1F).

Successful HSCGT at 4-months in MPSII animals

Given that neuropathology was similar between 2- and 4-month old mice, an identical LV.IDS HSCGT approach to that described previously in 2-month old animals[12] was performed into 4-month old MPSII animals to determine the efficacy of HSCGT therapy with later treatment. Lineage-depleted MPSII bone marrow was transduced with LV.IDS and transplanted into busulfan-conditioned 16-week-old MPS II mouse recipients (Fig S2A). Donor chimerism was monitored at 6-months of age, behaviour tests and X-rays were performed at 8-months of age and animals were sacrificed for biochemical and histological analysis at 9-months of age. Analysis of tissues from these animals were directly compared to results achieved in the previous study where MPSII mice were transplanted at 2-months of age. Donor chimerism

in 4-month-old transplanted animals was measured at 85% (range 74% to 94%; Fig S2B), similar to chimerism values achieved in younger animals (average 88%; range 84% to 92%).

Late LV.IDS HSCGT still provides supra-physiological levels of active IDS in peripheral organs but displays lower efficiency in the brain

Vector copy number (VCN) and IDS enzyme activity was measured in MPSII animals treated at 4-months of age throughout the body and compared with previous results achieved following transplant at 2-months of age. Measured VCN was equivalent between transplant groups in many organs apart from the bone marrow, where a significant increase in VCN was seen in the 2-month HSCGT group compared to 4-month group and similarly there was a small increase in VCN in the lungs of 2-month-old treated mice. Conversely, higher VCN values were observed in the brain of 4-month-old treated mice (0.06), when compared to 2-month old treated animals (0.03) (Fig 2A).

Supraphysiological enzyme was achieved in all peripheral organs of LV.IDS 4-month treated MPSII animals, with a 10-fold increase in IDS enzyme in the bone marrow, 13.5-fold increase in plasma and 4.9-fold increase in the spleen compared to WT. In the brain 1.1% of WT IDS levels were achieved following HSCGT at 4-months. IDS enzyme levels achieved from a late transplant at 4-months of age were comparable to levels achieved following transplant at 2-months of age in peripheral tissues including the bone marrow, spleen and liver (Fig 2B-F). However central levels of enzyme in the brain were decreased (1.1% following a 4-month versus 3.4% achieved following a 2- month transplant; Fig 2G).

Late transplant decreases HS storage both peripherally and centrally, yet sulphation status of the HS chain remains high

To determine the efficiency of IDS enzyme in transplanted animals at eliminating storage material, HS was measured peripherally in liver tissue and centrally in the brain (Fig 3). In the liver, HSCGT at 4-months resulted in effective normalisation of HS levels to WT (Fig 3A), with coincident restoration of HS disaccharide patterning (Fig 3B). In the brain, a significant 1.8-fold reduction in HS levels was achieved following late transplant, which was equivalent to the levels of reduction achieved by transplant at 2-months of age (Fig 3C). However, when the patterning of the HS chain was studied, the effectiveness of the later transplant was

10

reduced compared to early treatment, with significant increases in the most sulphated disaccharide types in 4-month treated animals (Fig 3D).

Late HSCGT appears to be less effective at reducing neuropathology in MPSII mice

Given the extensive neuropathology in mice at 2-months of age and similarities between animals at 2- and 4-months of age (Fig 1), staining for GFAP, LAMP2 and ISB4 was performed in the brains of control and 2- or 4-month HSCGT-treated animals at harvest (Fig 4 and 5). Following HSCGT, staining for LAMP2 and GFAP suggested that HSCGT either early or late could effectively reduce lysosomal swelling to near WT levels in the cortex region of the brain (Fig 4A/B). However, in other regions of the brain including the striatum, reductions of approximately 50% compared to untreated MPSII animals were apparent (Fig 4C), with levels remaining elevated over WT.

Astrocytosis remained evident in HSCGT-treated animals, with clear astrocytic activation in all regions of the brain studied (Fig 4A), yet they were noticeably reduced compared to untreated MPSII animals. Reductions in astrocytosis were more pronounced with earlier treatment (Fig 4D/E), however there was no significant difference between 2- and 4-month HSCGT-treated animals.

Activated microglial cells were also abundant in 2- and 4-month HSCGT-treated animals. 2-month HSCGT-treatment improved outcomes in 3 out of 4 brain regions over untreated MPSII controls, whilst mice treated at 4-months were not significantly different to MPSII untreated controls in any brain region (Fig 5). A trend towards increased reversibility of neuropathology was apparent with early treatment, but no significant differences were measured between 2- and 4-month HSCGT-treated groups (Fig 5B-E).

The extensive neuropathology observed in MPSII patients usually results in severe behavioural problems. When comparing 2- and 4-month HSCGT, neither treatment was able to correct the existing spatial working memory deficits present in MPSII animals (Fig 5G), although this was expected based on the relatively low enzyme activity data in the brain (Fig 2G).

11

Reversal of bone abnormalities and sensorimotor coordination following LV.IDS-HSCGT at 4-months of age

All MPSII patients exhibit significant skeletal abnormalities and limited joint motility, which can be modelled in MPSII animals. In order to evaluate the somatic efficacy of HSGCT, skeletal abnormalities were assessed using total body X-rays at 8-months of age (6- or 4-months post-LV.IDS-HSCGT). MPSII animals exhibit measurable thickening in the width of the zygomatic arches in the skull and the humerus and femur bones (Fig 6) which previously has been shown to be noticeable as early as 2-months of age[20]. Complete reversal of these abnormalities in the cheekbones and femur were obtained with both early and late LV.IDS-HSCGT treatment, with bone width in these treated animals indistinguishable from WT (Fig 6A/B/E/F). A significant decrease in width of the humerus compared to untreated MPSII was also seen in both HSCGT-treated groups (Fig 6C/D). To investigate the functional outcomes of therapy, sensorimotor coordination was measured using an accelerating rotarod apparatus at 6- or 4-months post-transplant/8-months of age (Fig 6G). Compared to MPSII animals, both LV.IDS-HSCGT MPSII groups showed equivalent increases in performance on the accelerating rod (Fig 6H). It is noted that WT animals performed only marginally better than untreated MPSII animals, likely due to visible weight gain in WT animals at 8-months of age, similar to previous results[20].

Discussion

Currently, finding a suitable therapeutic option to address neuropathic MPS diseases is still a challenging field. While ERT has proved to be a suitable option to rescue the somatic symptoms associated with MPSII[21], HSCGT provides a promising therapy to treat the brain[16,17], although time of intervention might still pose a threat to its efficacy. In MPSI patients, HSCT is typically given to patients before the age of two, with the benefit from HSCT treatment decreasing proportional to transplant age[22]. After this age, reductions in efficacy in the brain, versus the risk of complications from HSCT treatment, preclude this treatment option. Thus, in this study, MPSII disease progression was investigated to elucidate optimal therapeutic windows.

12

Using the MPSII mouse model we set out to determine the degree of brain HS storage and neuropathology in 2- (young), 4- (middle-aged) and 9-month (old) animals. Here we have demonstrated that significant neurodegeneration due to accumulation of highly sulphated HS and presumably other secondary storage materials were evident in MPSII animals by 2-months of age, prior to delivery of HSCGT. Notably, a significant increase in HS accumulation was observed in the brain between 2 and 9 months of age, which was complemented by progressive enlargement of the lysosomal compartment. However, changes in sulphation patterning, as well as glial activation, seemed to mostly occur prior to 2 months of age. This could be explained by the fact that accumulation of highly sulphated GAGs potentially triggers neuroinflammation through Toll-like receptor 4 (TLR4) binding, a receptor which is present on the surface of microglia, ultimately determining its activation. Once activated, microglia are known to produce several pro-inflammatory cytokines, such as IL-1β, IL-6, and TNF-α, which can further drive astrogliosis and potentially neuronal degeneration[23,24]. While the high level of neuroinflammation observed in the MPSII mice matches the significant neuroinflammatory burden that may be manifesting as an early developmental delay in MPSII children[25], mouse models of MPSI, IIIA and IIIB displayed a slower progression of neuropathology, with astrogliosis and microgliosis reaching a peak at 9 months of age[26].

As would be expected based on the progressive nature of the disease, early HSCGT was predicted to be far more effective than later treatment. Our results indicate that while this is true for CNS pathology, somatic disease can be equally reversed when delivering HSCGT at 4 months of age. In fact, somatic tissues were largely undistinguishable between early and late HSCGT-treated groups, despite the differences in length of treatment of animals at the time of comparison (early animals treated at 2-months are 6-months post-therapy, whereas animals treated later at 4-months are only 4-months post-therapy). Notably, similar levels of lysosomal enzyme delivery to bone marrow and peripheral tissues were achieved when comparing the two treatments; these levels were also comparable to the ones reported following early HSCGT in other MPS disorders[9,10]. Bone-abnormalities are considered one of the trickiest aspects of disease to treat, presumably due to limited enzyme penetration into musculoskeletal tissues due to limited blood flow[29]. Equally bone damage may be too extensive for repair. Significantly, late HSCGT provided full recovery of the bone defect

13

apparent at the time of treatment[20] both at a structural (skeletal defects) and functional (sensorimotor coordination) level, with increased benefits when compared to late ERT[30]. ERT is not only costly but also restrictive to patients, requiring a lifelong commitment to weekly intravenous enzyme delivery, often in the clinic. Thus, a one-shot HSCGT therapy, resulting in significantly increased delivery of the missing enzyme to peripheral tissues compared to standard HSCT, may offer significant benefit for older MPSII patients. It is of course possible that we are not measuring subtle enough outcomes to determine if somatic disease is completely corrected by either treatment, and notably we did not look at cardiac outcomes in this study, a notable manifestation of disease in patients.

With regards to CNS pathology, the percentage of WT brain IDS enzyme achieved trended lower in animals treated at 4-months of age compared to 2-months. This was complemented by poorer correction of HS sulphation patterning and gliosis levels. On the other hand, similar reductions in brain HS and lysosomal swelling, and cerebellar function normalisation were observed following both treatments. This is in line with the neurologic recovery observed in both MPS I and MPS II mice when treated at advanced disease stages with AAV9 vector administered intracerebroventricularly and intravenously[28,29]. There are many possible reasons for the decrease in CNS enzyme expression. Firstly, lower recorded VCN in the bone marrow of the 4-month treated HSCGT group may account for the difference in brain enzyme. In this regard, defects in homing and migration pathways have been observed in a mouse model of MPSIH[30], resulting in decreased engraftment following HSCT. This was proved to be caused by highly sulphated HS-mediated sequestration of multiple cytokines and chemokines, such as CXCL12. The latter is in fact a key mediator of HSC homing to the bone marrow following transplant, and it normally relies on HS as a coreceptor to bind its cognate ligand. Notably, in MPSIH, sequestration of CXCL12 seems to be caused by excessive accumulation of 2-O-sulfated HS, for which the chemokine already has a binding preference under normal conditions. Although this has not been investigated yet, highly sulphated HS may play a similar role in other MPS subtypes, such as MPSII. In this respect, our analysis of disease progression indicates HS progressive accumulation between 2 and 9 months of age, inevitably resulting in an increase of its sulphated forms. As a result, delaying the time of therapeutic intervention might have repercussions on the homing of hematopoietic

14

progenitors to bone marrow, following transplant. In a similar way, increased accumulation of highly sulphated HS might also alter key signalling pathways involved in the migration of engrafted monocytes to the brain, resulting in reduced brain enzyme, and eventually reduced disease correction.

In addition, it should be also noted that as stated above, there are differences in time post-transplant between groups (4- versus 6-months in late versus early treated animals respectively), thus enzyme levels may rise further with increased time post-transplant as further migration may occur. Finally, increased neuronal damage in the brain may alter the survival of engrafting cells, reducing the level of enzyme expression.

On the one hand, our results imply a clear benefit from HSCGT with both early and late transplant and provide a clear advantage of late HSCGT as a one-time therapy over ERT for somatic organs. On the other hand, our data suggest reduced correction of brain pathology following late HSCGT, hence supporting the view that the earlier the patients are treated, the better the overall therapeutic outcome.

Acknowledgements

Authors' contributions

O.M. performed the majority of the *in vitro* experiments and wrote the paper. **A.L.** performed the majority of the *in vivo* work. **E.S.** helped with *in vitro* experiments. **C.O.L** helped with *in vivo* work. **R.H** supervised the project, helped with *in vivo* work, reviewed the data analysis and made the figures. **B.W.B.** conceptualised the project, acquired fundings, supervised the project and contributed to writing and reviewed the paper.

Authors' disclosure

The authors report no conflict of interest.

15

Funding statement

16

References

1. Boustany R-MN. Lysosomal storage diseases—the horizon expands. Nat Rev Neurol 2013;9(10):583–598; doi: 10.1038/nrneurol.2013.163.

2. Clarke LA. The mucopolysaccharidoses: a success of molecular medicine. Expert Rev Mol Med 2008;10:e1; doi: 10.1017/S1462399408000550.

3. Gupta R, Bhushan Pandey C, Tripathi S. Mucopolysaccharidosis type II (Hunter's syndrome) e A clinical case report. J Indian Coll Cardiol 2015;5:61–66; doi: 10.1016/j.jicc.2014.07.004.

4. Wraith JE, Scarpa M, Beck M, et al. Mucopolysaccharidosis type II (Hunter syndrome): a clinical review and recommendations for treatment in the era of enzyme replacement therapy. Eur J Pediatr 2008;167(3):267–77; doi: 10.1007/s00431-007-0635-4.

5. Whiteman DA, Kimura A. Development of idursulfase therapy for mucopolysaccharidosis type II (Hunter syndrome): the past, the present and the future. Drug Des Devel Ther 2017;11:2467–2480; doi: 10.2147/DDDT.S139601.

6. Fraldi A, Serafini M, Sorrentino NC, et al. Gene therapy for mucopolysaccharidoses: in vivo and ex vivo approaches. Ital J Pediatr 2018;44(Suppl 2):130; doi: 10.1186/s13052-018-0565-y.

7. Holley RJ, Wood SR, Bigger BW. Delivering Hematopoietic Stem Cell Gene Therapy Treatments for Neurological Lysosomal Diseases. 2018; doi: 10.1021/acschemneuro.8b00408.

8. Hoogerbrugge PM, Suzuki K, Suzuki K, et al. Donor-Derived Cells in the Central Nervous System of Twitcher Mice After Bone Marrow Transplantation. Science (80-) 1988;239(4843):1035–1038; doi: 10.1126/SCIENCE.3278379.

17

9. Capotondo A, Milazzo R, Politi LS, et al. Brain conditioning is instrumental for successful microglia reconstitution following hematopoietic stem cell transplantation. Proc Natl Acad Sci U S A 2012;109(37):15018–15023; doi: 10.1073/PNAS.1205858109.

10. Sergijenko A, Langford-Smith A, Liao AY, et al. Myeloid/Microglial Driven Autologous Hematopoietic Stem Cell Gene Therapy Corrects a Neuronopathic Lysosomal Disease. Mol Ther 2013;21(10):1938–1949; doi: 10.1038/mt.2013.141.

11. Gleitz HF, Liao AY, Cook JR, et al. Brain-targeted stem cell gene therapy corrects mucopolysaccharidosis type II via multiple mechanisms. EMBO Mol Med 2018;10(7):e8730; doi: 10.15252/emmm.201708730.

12. Holley RJ, Ellison SM, Fil D, et al. Macrophage enzyme and reduced inflammation drive brain correction of mucopolysaccharidosis IIIB by stem cell gene therapy. Brain 2018;141(1):99–116; doi: 10.1093/brain/awx311.

13. Barth AL, de Magalhães TSPC, Reis ABR, et al. Early hematopoietic stem cell transplantation in a patient with severe mucopolysaccharidosis II: A 7 years follow-up. Mol Genet Metab reports 2017;12:62–68; doi: 10.1016/j.ymgmr.2017.05.010.

14. Kubaski F, Yabe H, Suzuki Y, et al. Hematopoietic Stem Cell Transplantation for Patients with Mucopolysaccharidosis II. Biol Blood Marrow Transplant 2017;23(10):1795–1803; doi: 10.1016/J.BBMT.2017.06.020.

15. Biffi A. Hematopoietic Stem Cell Gene Therapy for Storage Disease: Current and New Indications. Mol Ther 2017;25(5):1155–1162; doi: 10.1016/j.ymthe.2017.03.025.

16. Hofling AA, Vogler C, Creer MH, et al. Engraftment of human CD34+ cells leads to widespread distribution of donor-derived cells and correction of tissue pathology in a novel murine xenotransplantation model of lysosomal storage disease. Blood 2003;101(5):2054–2063; doi: 10.1182/BLOOD-2002-08-2597.

18

17. Hofling AA, Devine S, Vogler C, et al. Human CD34+ hematopoietic progenitor cell-directed lentiviral-mediated gene therapy in a xenotransplantation model of lysosomal storage disease. Mol Ther 2004;9(6):856–65; doi: 10.1016/j.ymthe.2004.03.013.

18. Wakabayashi T, Shimada Y, Akiyama K, et al. Hematopoietic Stem Cell Gene Therapy Corrects Neuropathic Phenotype in Murine Model of Mucopolysaccharidosis Type II. Hum Gene Ther 2015;26(6):357–366; doi: 10.1089/hum.2014.158.

19. Langford-Smith A, Wilkinson FL, Langford-Smith KJ, et al. Hematopoietic stem cell and gene therapy corrects primary neuropathology and behavior in mucopolysaccharidosis IIIA mice. Mol Ther 2012;20(8):1610–21; doi: 10.1038/mt.2012.82.

20. Gleitz HFE, O'Leary C, Holley RJ, et al. Identification of age-dependent motor and neuropsychological behavioural abnormalities in a mouse model of Mucopolysaccharidosis Type II. Ginsberg SD. ed. PLoS One 2017;12(2):e0172435; doi: 10.1371/journal.pone.0172435.

21. Muenzer J, Botha J, Harmatz P, et al. Evaluation of the long-term treatment effects of intravenous idursulfase in patients with mucopolysaccharidosis II (MPS II) using statistical modeling: data from the Hunter Outcome Survey (HOS). Orphanet J Rare Dis 2021;16(1):1–14; doi: 10.1186/S13023-021-02052-4/FIGURES/6.

22. Taylor M, Khan S, Stapleton M, et al. Hematopoietic stem cell transplantation for mucopolysaccharidoses; past, present, and future. Biol Blood Marrow Transplant 2019;25(7):e226; doi: 10.1016/J.BBMT.2019.02.012.

23. Parker H, Bigger BW. The role of innate immunity in mucopolysaccharide diseases. J Neurochem 2019;148(5):639–651; doi: 10.1111/jnc.14632.

24. Mandolfo O, Parker H, Bigger B. Innate Immunity in Mucopolysaccharide Diseases. Int J Mol Sci 2022, Vol 23, Page 1999 2022;23(4):1999; doi: 10.3390/IJMS23041999.

19

25.   Roberts J, Stewart C, Kearney S. Management of the behavioural manifestations of Hunter syndrome. Br J Nurs 2016;25(1):22–30; doi: 10.12968/bjon.2016.25.1.22.

26.   Wilkinson FL, Holley RJ, Langford-Smith KJ, et al. Neuropathology in mouse models of mucopolysaccharidosis type I, IIIA and IIIB. PLoS One 2012;7(4):e35787; doi: 10.1371/journal.pone.0035787.

27.   Tomatsu S, Azario I, Sawamoto K, et al. Neonatal cellular and gene therapies for mucopolysaccharidoses: the earlier the better? J Inherit Metab Dis 2016;39(2):189–202; doi: 10.1007/s10545-015-9900-2.

28.   Podetz-Pedersen KM, Laoharawee K, Singh S, et al. Neurologic Recovery in MPS i and MPS II Mice by AAV9-Mediated Gene Transfer to the CNS after the Development of Cognitive Dysfunction. Hum Gene Ther 2023;34(1–2):8–18; doi: 10.1089/HUM.2022.162/ASSET/IMAGES/LARGE/HUM.2022.162_FIGURE6.JPEG.

29.   Fu H, Zaraspe K, Murakami N, et al. Targeting Root Cause by Systemic scAAV9-hIDS Gene Delivery: Functional Correction and Reversal of Severe MPS II in Mice. Mol Ther - Methods Clin Dev 2018;10:327–340; doi: 10.1016/j.omtm.2018.07.005.

30.   Watson HA, Holley RJ, Langford-Smith KJ, et al. Heparan sulfate inhibits hematopoietic stem and progenitor cell migration and engraftment in mucopolysaccharidosis I. J Biol Chem 2014;289(52):36194–36203; doi: 10.1074/JBC.M114.599944.
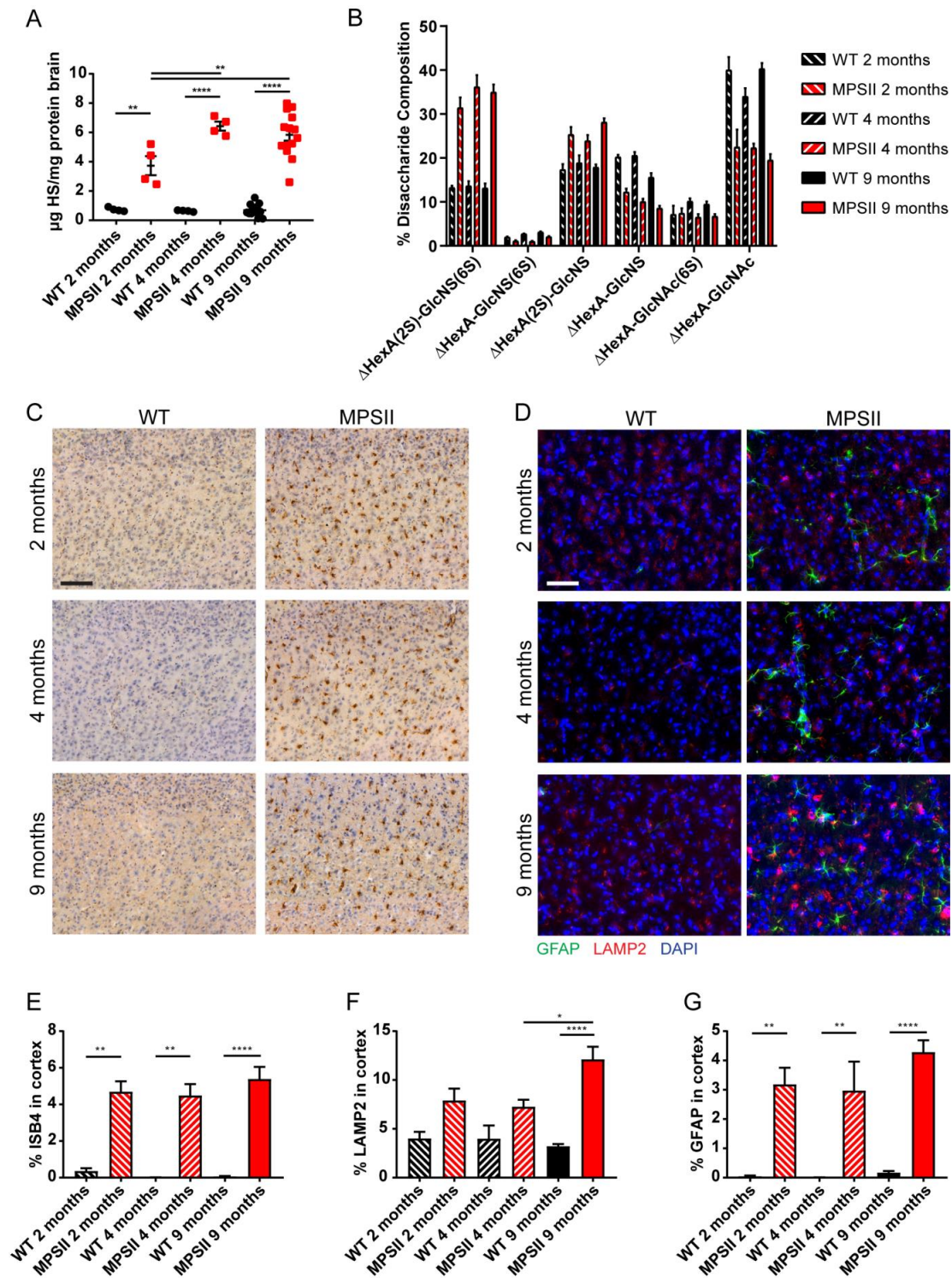
Figure legends

Figure 1: Significant pathological accumulation of HS and neuropathology is evident in 2-months old MPSII mice with progression seen with age.

A: HS quantification from the brains of WT and MPSII mice at 2-, 4- and 9-months of age (n=4-14 per group) measured at micrograms HS per milligram of total brain protein. Individual mice from each group are plotted.

B: Compositional disaccharide analysis of HS chains from the brains of WT and MPSII mice at 2-, 4- and 9-months of age quantified in A.

C: Representative sections of positively stained microglia (isolectin B4, brown) at 2-, 4- and 9-months of age covering cortical layer IV/V/VI (-0.82 relative to Bregma). Sections were counterstained with Mayer's haematoxylin to highlight the nuclei (purple). Scale bar = 100µm.

D: Representative sections of the brain stained with LAMP2 (red), GFAP (green), and DAPI (blue) covering cortical layer IV/V/VI (-0.82 relative to Bregma). Scale bar = 50µm.

E: Quantification of isolectin B4 (ISB4) staining in cortical layer IV/V/VI (-0.82 relative to Bregma) plotting percentage area positively stained in all animals.

F: Quantification of LAMP2 staining in cortical layer IV/V/VI (-0.82 relative to Bregma) plotting percentage area positively stained in all animals.

G: Quantification of GFAP staining in cortical layer IV/V/VI (-0.82 relative to Bregma) plotting percentage area positively stained in all animals.

Error bars represent SEM. Significant differences are shown with a line and were calculated using a one-way ANOVA using Tukey post hoc test, $*P < 0.05$, $**P < 0.01$, $***P < 0.001$ and $****P < 0.0001$.
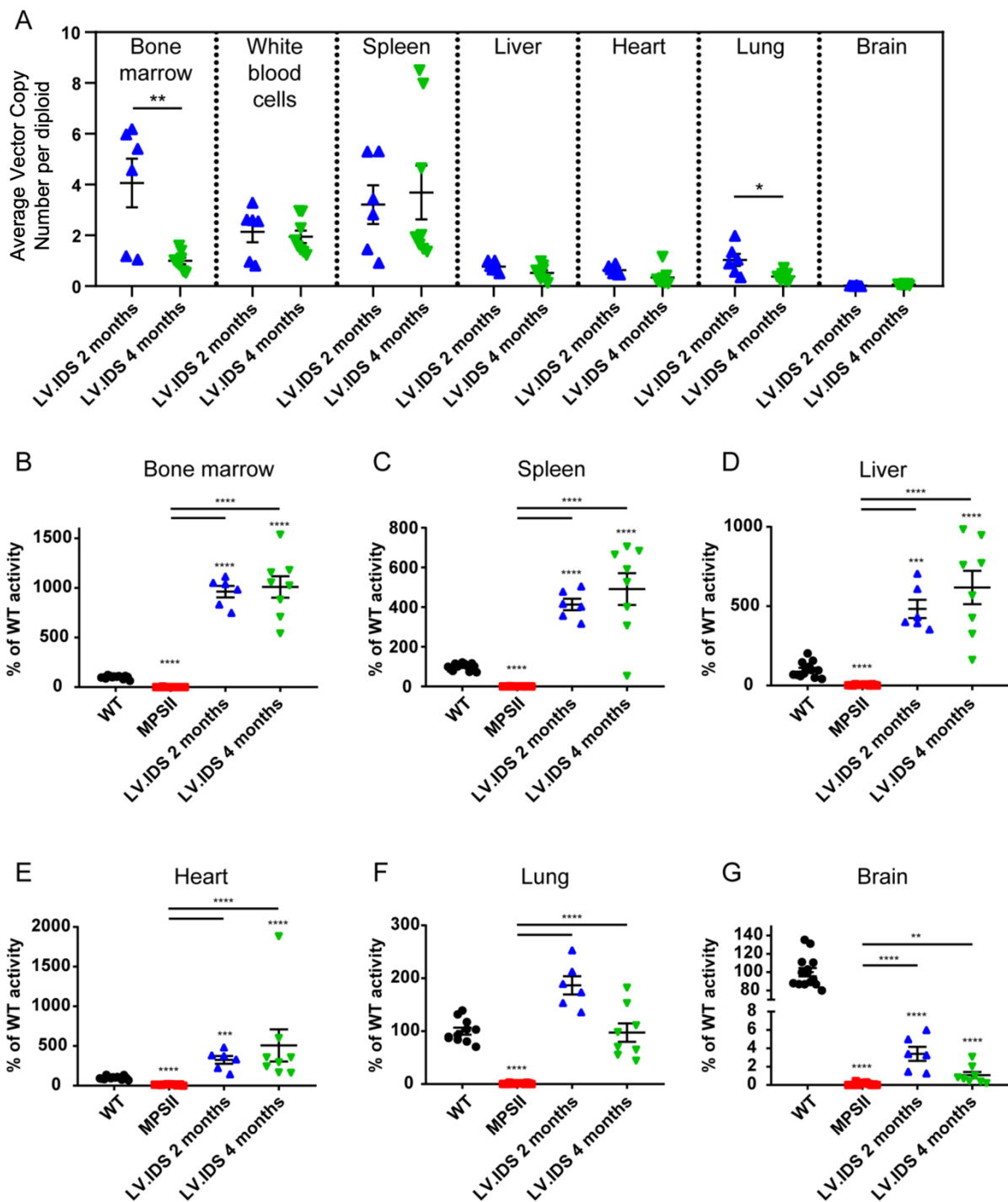
Figure 2: Late LV.IDS HSCGT treatment is equivalent to earlier treatment in peripheral tissues, however enzyme levels achieved in the brain are decreased.

A: Vector copy number measured in the organs of MPSII animals treated with LV.IDS at either 2- or 4-months of age. Error bars represent SEM. Significant differences were calculated using an unpaired T-test, *P < 0.05, **P < 0.01.

23

B-G: IDS enzyme levels measured in the bone marrow (B), spleen (C), liver (D), heart (E), Lung (F) and brain (G) at 9-months of age in control animals or following LV.IDS HSCGT at either 2- or 4-months of age. Data are shown as the percentage of WT enzyme. Error bars represent SEM. Significant differences were calculated using a one-way ANOVA, *P < 0.05, **P < 0.01, ***P < 0.001 and ****P < 0.0001. Significance to WT is shown above recorded data, all other comparisons are shown with a line.
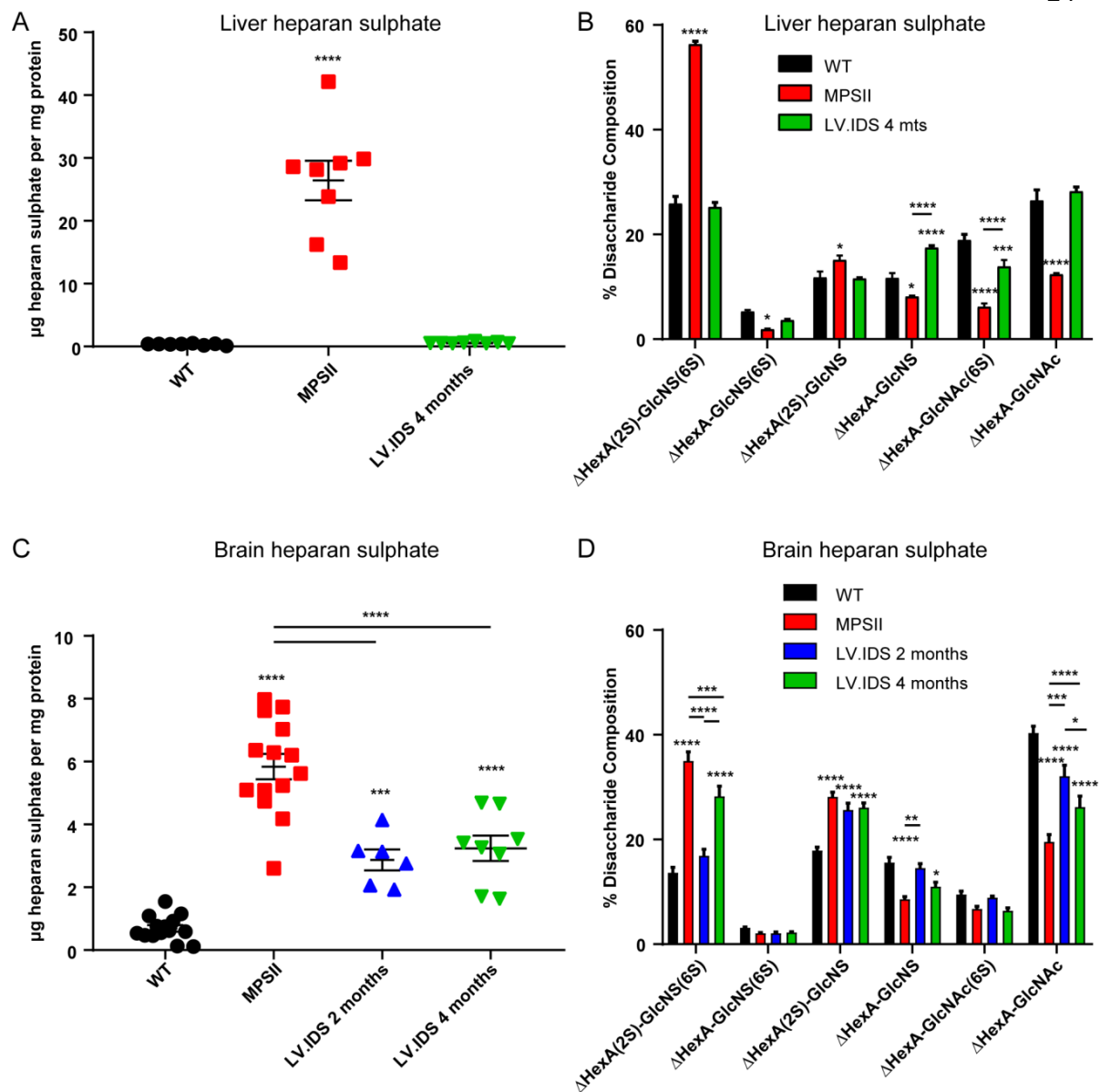
24

Figure 3: Late LV.IDS treatment effectively decreases HS burden in peripheral and central tissues, but fails to correct disaccharide patterning in the brain.

A: HS quantification in the liver at 9-months of age of control and MPSII mice treated with LV.IDS from 4-months of age.

B: Percentage contribution of each disaccharide type that makes up the HS chain in the liver at 9-months of age of control and MPSII mice treated with LV.IDS from 4-months of age.

25

C: HS quantification in the brain at 9-months of age of control and MPSII mice treated with LV.IDS from 2- or 4-months of age.

D: Percentage contribution of each disaccharide type that makes up the HS chain in the brain at 9-months of age of control and MPSII mice treated with LV.IDS from 2- or 4-months of age.

Error bars represent SEM. Significant differences were calculated using a one-way ANOVA, *$P < 0.05$, **$P < 0.01$, ***$P < 0.001$ and ****$P < 0.0001$. Significance to WT is shown above recorded data, all other comparisons are shown with a line.
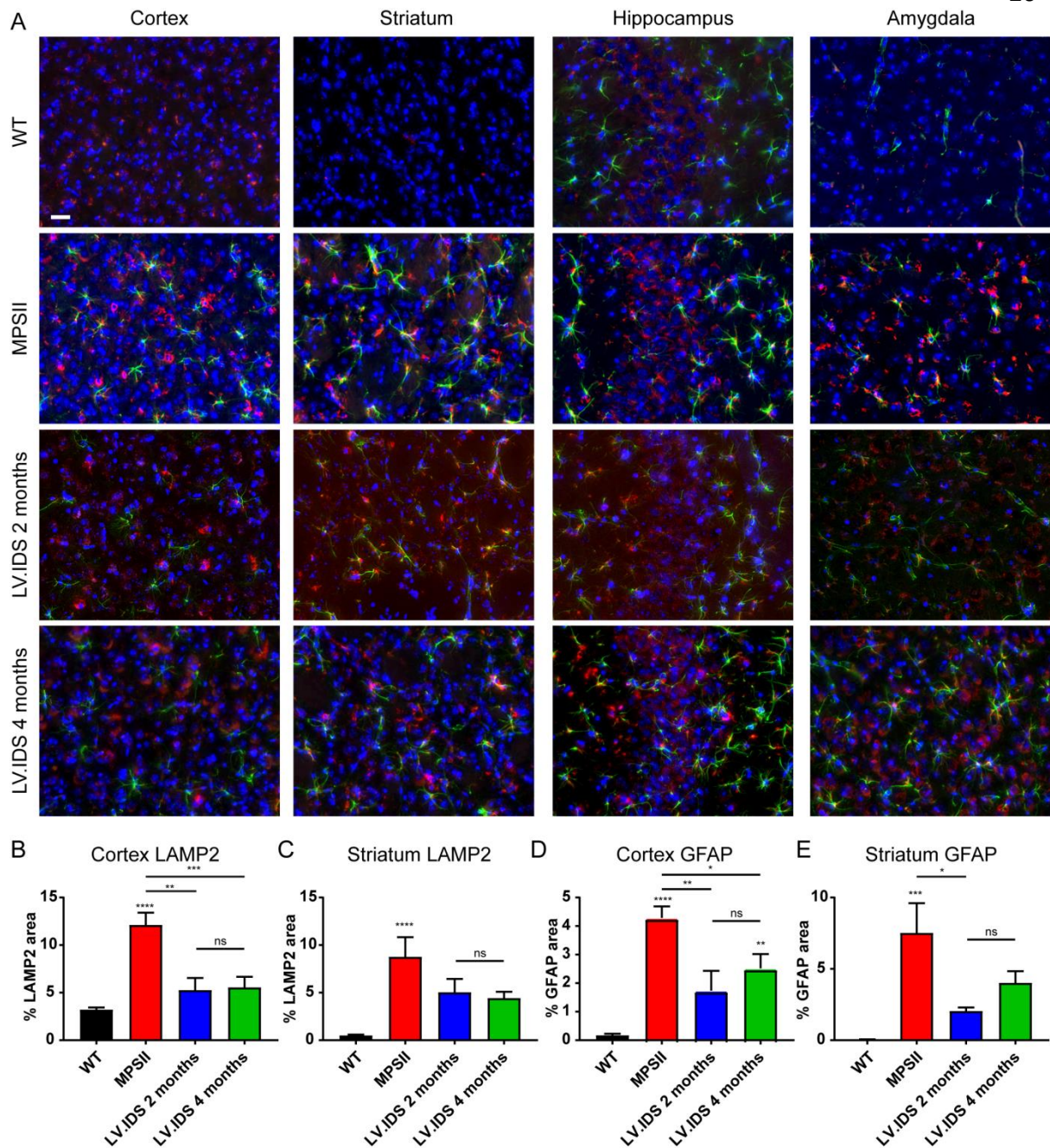
Figure 4: late LV.IDS treatment reduces astrocytosis and lysosomal swelling in the brain.

A: Representative images of the indicated region of the brain stained with GFAP (green), LAMP2 (red) and DAPI (nucleus, blue). Images correspond to cortical layers IV/V/VI (-0.82 relative to Bregma), striatum (0.14 relative to Bregma), hippocampus CA3 (-1.7 relative to Bregma), and amygdala (-1.7 relative to Bregma) regions from control and LV.IDS-treated mice at 2- and 4-months of age. Scale bar = 50µm.

27

B/C: Percentage area stained with LAMP2 from each field of view in the cortex (B) and striatum (C) from control and LV.IDS-treated mice at 2- and 4-months of age.

D/E: Percentage area stained with GFAP from each field of view in the cortex (D) or striatum (E) from control and LV.IDS-treated mice at 2- and 4-months of age.

Error bars represent SEM. Significant differences were calculated using a one-way ANOVA, *$P < 0.05$, **$P < 0.01$, ***$P < 0.001$ and ****$P < 0.0001$. Significance against WT is shown above recorded data, all other comparisons are shown with a line.
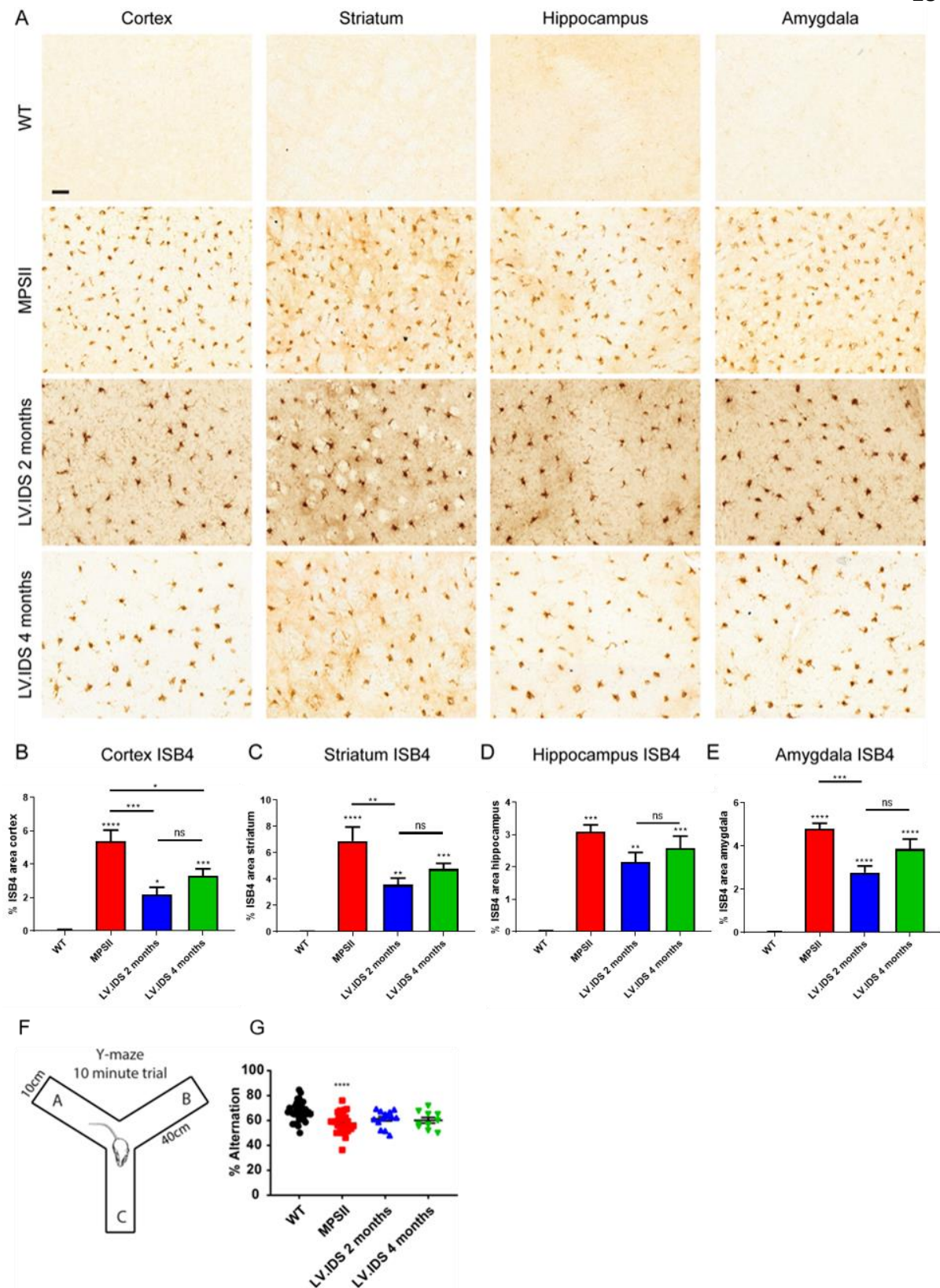
28

Figure 5: Late LV.IDS reduces microgliosis in MPSII mice, but does not improve behaviour.

29

A: Representative images of the indicated region of the brain stained with ISB4 (brown). Images correspond to cortical layers IV/V/VI (-0.82 relative to Bregma), striatum (0.14 relative to Bregma), hippocampus CA3 (-1.7 relative to Bregma), and amygdala (-1.7 relative to Bregma) regions from control or MPSII HSCGT-treated mice at 2- and 4-months of age. Scale bar = 100μm.

B-E: Relative quantification of ISB4+ cells using ImageJ software in the cortex (B), striatum (C), hippocampus (D) and amygdala (E).

F: Schematic of the Y-maze, with three identical arms. The mouse is placed in the centre of the maze and allowed to explore freely for 10 minutes. Entry with all four paws into each arm of the maze, A, B or C is recorded.

G: At 8 months of age, both control and treated mice underwent working memory testing in the Y-maze. The percentage alternation between arms of the maze is shown.

Data are presented as mean ± SEM. Significant differences were calculated using a one-way ANOVA, *$P < 0.05$, **$P < 0.01$, ***$P < 0.001$ and ****$P < 0.0001$. Significance against WT is shown above recorded data, all other comparisons are shown with a line.
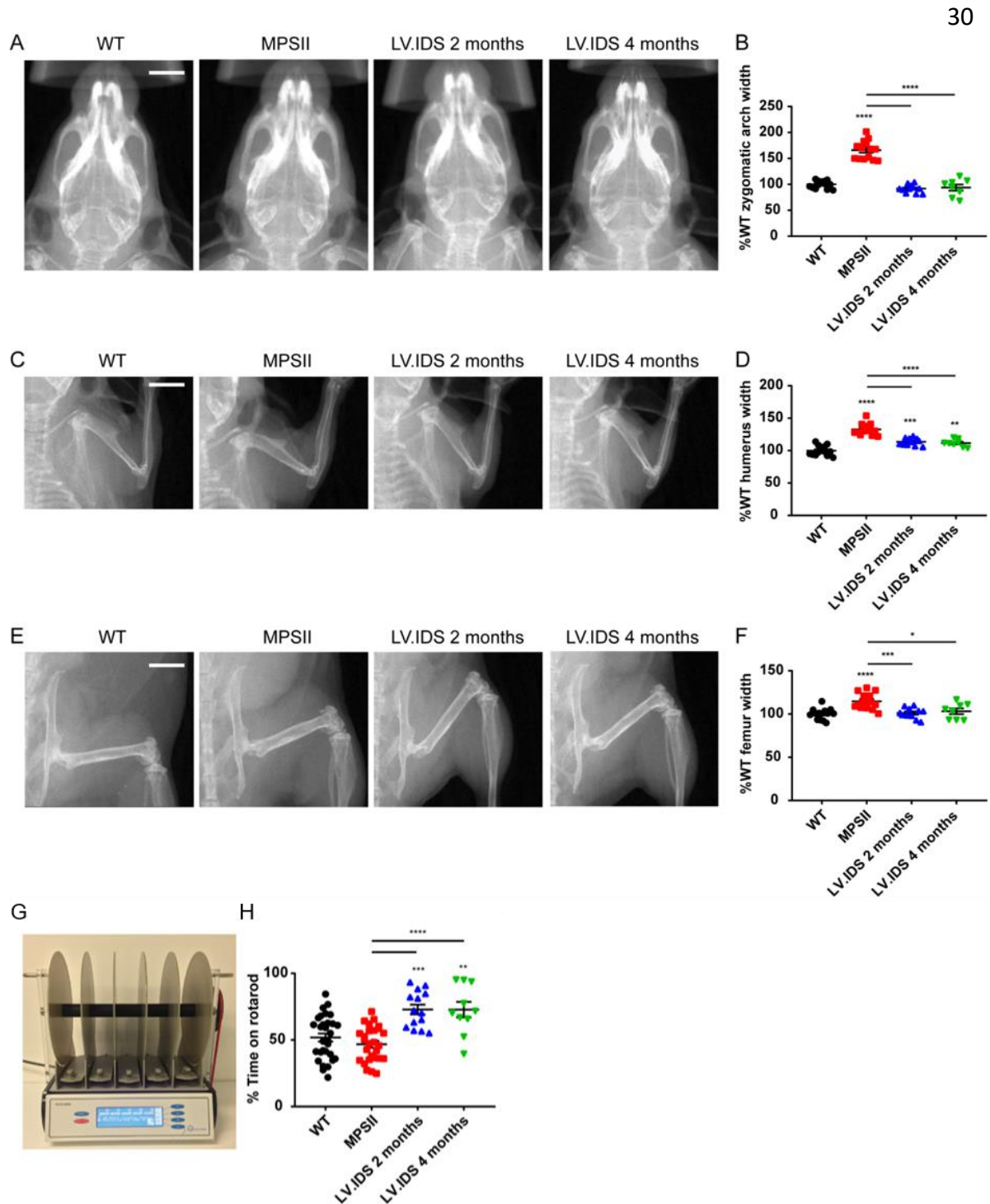
30

Figure 6: Late LV.IDS treatment effectively treats skeletal defects in MPSII mice

A: Representative X-ray images of control and treated MPSII mouse craniums at 8-months of age.

B: Measurements of the zygomatic arch widths of control and treated mice.

31

C: Representative X-ray images of control and treated MPSII mouse humerus at 8-months of age.

D: Measurements of the humerus width of control and treated mice.

E: Representative X-ray images of control and treated MPSII mouse craniums at 8-months of age.

F: Measurements of the femur width of control and treated mice.

G: Rotarod apparatus.

H: At 8 months of age, both control and treated mice performed three trials on the accelerating rotarod for a maximum of 300 seconds. Percentage time spent on the rotarod as an average of the three trials is shown.

Error bars represent SEM. Significant differences were calculated using a one-way ANOVA, *$P < 0.05$, **$P < 0.01$, ***$P < 0.001$ and ****$P < 0.0001$. Significance against WT is shown above recorded data, all other comparisons are shown with a line.